Highlights on Spanish Astrophysics X, Proceedings of the XIII Scientific Meeting of the Spanish Astronomical Society held on July 16 – 20, 2018, in Salamanca, Spain. B. Montesinos, A. Asensio Ramos, F. Buitrago, R. Schödel, E. Villaver, S. Pérez-Hoyos, I. Ordóñez-Etxeberria (eds.), 2019

Kinematic structure in the Solar Neighbourhood and surroundings with *Gaia*: a vast richness to explore.

P. Ramos, T. Antoja, and F. Figueras

Dept. FQA, Institut de Ciències del Cosmos (ICCUB), Universitat de Barcelona (IEEC-UB), Martí Franquès 1, E08028 Barcelona, Spain

Abstract

Following from the recent second data release of the *Gaia* mission, we used the ∼5 million stars with high-quality six-dimensional phase-space information in the catalogue to explore the kinematic substructure of different Galactic neighbourhoods, including our own. As a result, we obtain a precise characterisation of these structures in the solar neighbourhood and their evolution with Galactocentric distance. Some are seen to have nearly constant kinetic energy at a given volume (e.g. Sirius), while others evolve keeping their vertical angular momentum nearly unchanged (e.g. Hercules). This information yields valuable insight about their respective origins and thus on the dynamics of the Milky Way.

1 Introduction

One of the major goals of Galactic dynamics is to obtain a self-consistent model of the Milky Way (MW) that reproduces to high accuracy the distribution of observed stars both in position and velocity. This task, however, has proven to be utterly complex, in part due to the lack of information of our own galaxy and on the phase-space distribution. Now, with the *Gaia* mission [9], we have access to a wealth of data never seen before which opens new horizons for our understanding of the Milky Way.

In the past, some of the works in this field explored the phase-space by looking at the velocity distribution of stars in the solar neighbourhood (SN). Then, they tried to recreated the different kinematic structures it contains, like the moving groups (MG), by modelling the MW with a bar, spiral arms, or other non-axisymmetric components (see [1] and references therein). Nonetheless, the large degree of degeneracy between models at the SN demands a deeper exploration of phase-space by extending the study of the velocity plane to other Galactic neighbourhoods. This has only been possible just recently, being [2] the first to do so, followed by other authors (e.g., [20, 13]) that worked with increasingly better data.

The recent publication of the *Gaia* second data release (DR2) [8] entails an order of magnitude improvement over past surveys, both in quantity and quality. In this work, we present the results of using ∼5 millions stars with full 6D information to study the changes in the velocity distribution with Galactocentric radius and azimuth by means of the wavelet transformation (WT).

This talk is organised as follows. In Section 2, we summarise the main properties of the sample and outline the methods used for its exploitation. Then, in Section 3 we characterise the structures found at the SN to, afterwards, follow their evolution with Galactocentric distance and azimuth in Section 4. Finally, Section 5 contains a short discussion and the conclusions.

2 Methodology

The study of phase-space requires full 6D data, three coordinates for position and three for velocity. Therefore, from the whole *Gaia* DR2 catalogue, we selected those stars with parallax, proper motion and radial velocity. Furthermore, in order to use the inverse of the parallax as distance, we restricted ourselves to stars with small relative error ($\varpi/\sigma_\varpi \geq 5$) which mitigates the bias [5]. The sample we are left with is composed of 5,136,533 stars.

We used the Galactocentric cylindrical coordinates with the following constants: Sun at (R, ϕ, Z)=(8.34 kpc, 0°, 14 pc) [17, 6], peculiar velocity of the Sun of ($U_\odot$, $V_\odot$, $W_\odot$) = (11.1, 12.24, 7.25) $\mathrm{km\,s^{-1}}$ [18], and circular velocity for the Local Standard of Rest (LSR) of 240 $\mathrm{km\,s^{-1}}$ [17]. Consequently, we studied the velocity distributions in the Galactic plane ($|Z| < 500$ pc) with the variables $\dot{R} = V_R$ and $R\dot{\phi} = V_\phi$. We presented the density map of the sample in Fig. 1 of [16] along with the spatial distribution of the sub-samples used for the kinematic exploration. Each of these volumes is a portion of a cylinder with a width of 200 pc in Galactocentric radius and 3 degrees in azimuth, layout along the Sun-Galactic centre (GC) line from 6.04 kpc to 11.04 kpc every 100 pc.

Each volume in the sample is then decomposed into layers of different spatial frequencies (or sizes) using the WT. In particular, the *à trous* algorithm [19], which preserves the size of the original 2D image, in our case the histogram of the velocity plane, at each layer (or scale). At every pixel of each scale, the wavelet coefficient measures the degree of overdensity (positive coefficient) or underdensity (negative coefficient) compared to its 2^j closest neighbours, with j=0,1,..,J being the scale. In this sense, the WT highlights the structures of sizes between roughly $\Delta 2^j$ and $\Delta 2^{j+1}$, where Δ is the size of the pixels in the underlying histogram (for this work, 0.5 $\mathrm{km\,s^{-1}pixel^{-1}}$). Here, we focused on structures with sizes ∼4-8 $\mathrm{km\,s^{-1}}$ (j=3) and ∼8-16 $\mathrm{km\,s^{-1}}$ (j=4).

After calculating the wavelet coefficients, we performed a peak search and detected the local maxima which signals the location of different structures within the velocity distribution. Since these peaks are found in the wavelet space, we then performed an statistical evaluation of their significance with two indicators: Poisson noise, measured with the level of confidence at which the structure is likely to be real (C.L.= {0,1,2,3}), and Bootstrap noise, which measures the probability of having observed the peak in the data ($P_{BS} \in [0, 1]$). We say a

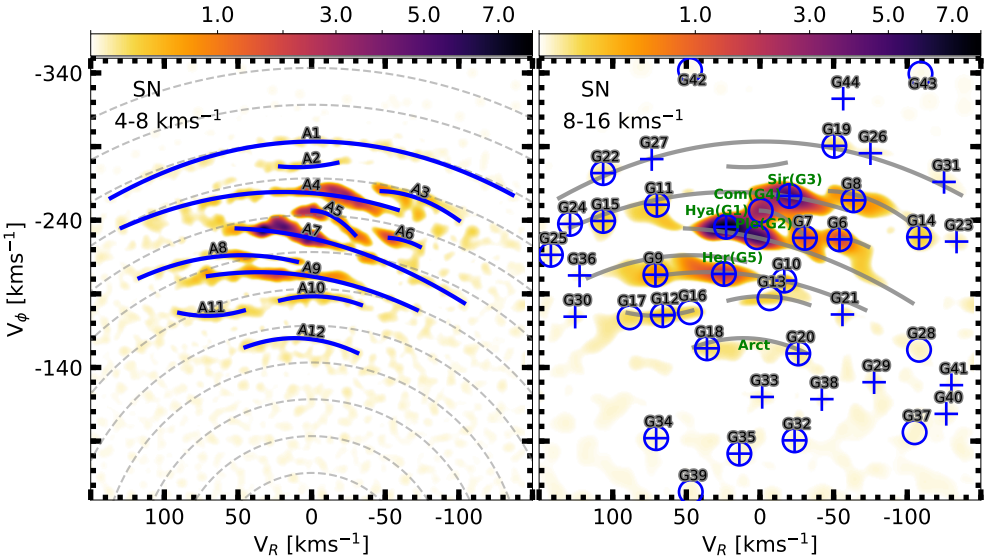

Figure 1: Wavelet coefficients of the velocity distribution at the SN. The structures found are shown for two different scales: arches at 4-8 km s^{-1} (left) and peaks at 8-16 km s^{-1} (right). For the former, dashed grey lines represent constant kinetic energy tracks. Circles on the right plot correspond to peaks that are significant according to Poisson noise (C.L.$\geq$2), while crosses correspond to those significant with respect to Bootstraps ($P_{BS} \geq 0.8$). Also, the arches found on the left panel are shown on the right panel as grey lines.

structure is significant if C.L.$\geq$2 or $P_{BS} \geq$0.8. For more details, see [16].

3 Solar neighbourhood

Figure 1 shows the result of applying the methodology described in the previous section to the sub-sample centred at the Sun's position (R$\in$[8.24, 8.44] kpc, $\phi \in$[-1.5,1.5] degrees). In particular, the wavelet scales corresponding to 4-8 km s^{-1} and 8-16 km s^{-1}. At the lower wavelet scale (left panel), we see that the coefficients are arranged in rather elongated structures and thus we chained the significant peaks found into arches (A1 to A12). The existence of such features in the velocity plane was already predicted based on alternative surveys by other authors (e.g., [1, 13]), yet with *Gaia* DR2 these can be seen simply by visual inspection of the histogram [11]. In fact, the prominent arch 1, which crosses the whole plane, was discovered for the first time in with this data [11]. [14, 12] showed that a disk out of equilibrium (e.g., by the close passage of a satellite galaxy) develops arch-like features of constant radial frequency due to phase mixing. Since the radial frequency mostly depends on the orbital energy [7], we plotted on the left panel of Fig.1 tracks of constant kinetic energy as dashed grey lines. In turn, this allows us to explain features such as A1 and A10. Other arches, like A4 (referred to as Sirius MG in the literature) can also be related to this dynamical mechanism knowing that the presence of a bar can cause some structures to deviate from symmetry [4].

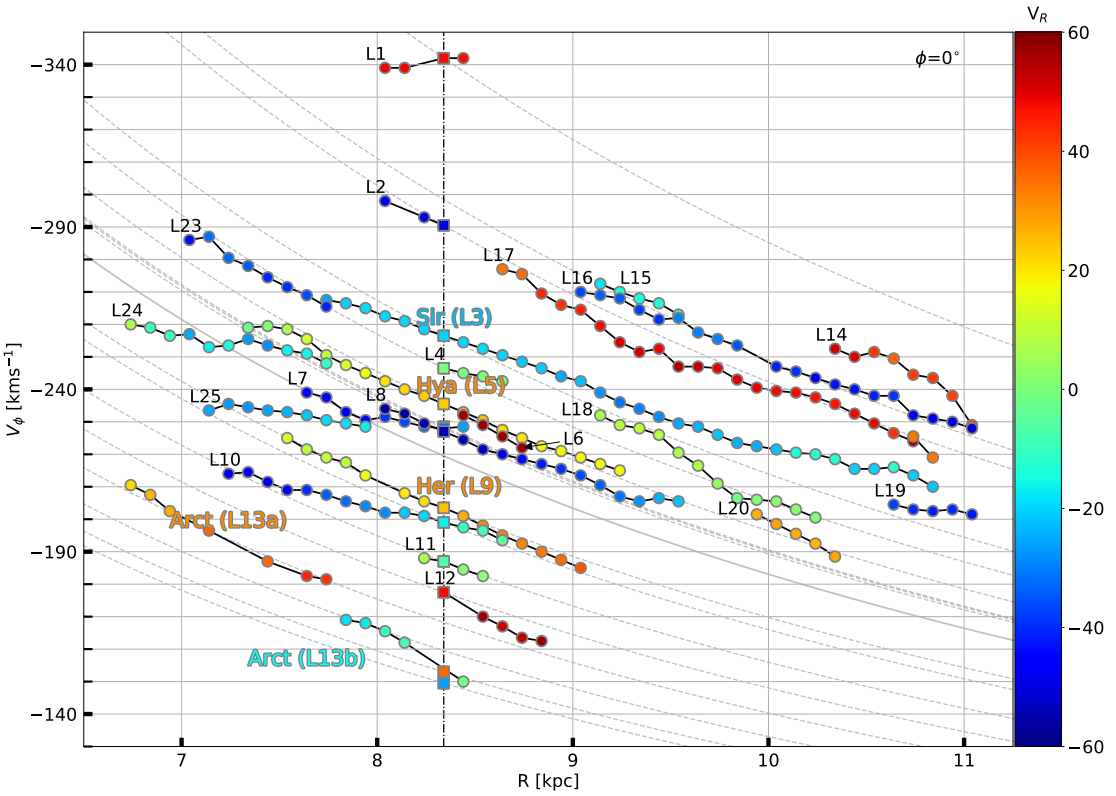

Figure 2: Evolution of the azimuthal velocity of the peaks with Galactocentric distance. The colour corresponds to the radial velocity, while the dashed grey lines are tracks of constant angular momentum. The dotted dashed line marks the position of the Sun. The names of relevant structures have been added for reference.

At the larger wavelet scale (8-16 km s^{-1}, right panel of Fig.1), the structures appear like rounded groups identified with circles (C.L.$\geq$2) and/or crosses ($P_{BS} \geq 0.8$). The well-known structures from the literature (Table C.1 from [16]) are all among the most prominent peaks in the sample. Still, we found $\sim$30 new candidates to MG. Whereas some have few stars and are significant solely due to their isolation, most are in fact produced by an elongated structure. When plotting the arches in the left panel on the right panel, we can see that some of the MGs are related to those features, such as Hercules (G5), G9 and G10 sitting on top of A9. Similarly, G16 (Bobylev16-22 and Arifyanto05, see [16] for more details) is related to G12 and G17, or G18 and G20 to the MG known as Arcturus.

4 Other Galactic neighbourhoods

After having analysed the SN, we performed an exhaustive search of peaks in the wavelet layer j=4 at all the Galactic neighbourhoods in the Sun-GC line, from 6.04 kpc to 11.04 kpc. As a result, we obtained a table with the velocity coordinates (V_R - V_ϕ) of each significant

overdensity in kinematic space and the corresponding Galactocentric distance (R) of the volume it was found in (see [16] for more figures and animations). After clustering together by eye the peaks according to their trend in R vs V_ϕ plane, and also taking into account V_R, we obtained a set of lines which are presented in Fig. 2. We observe that different structures follow distinct slopes but, on average, all of them fall at a rate of $\sim$23 $\mathrm{km\,s^{-1}kpc^{-1}}$, consistent with previous estimates [15].

Some structures, like Hercules (line 9), are most likely produced by a resonance. Such structures should evolve keeping the angular momentum roughly constant with radius, for small epicyclic amplitudes and to first order approximation [15]. Therefore, we plotted tracks of constant vertical angular momentum, L_z (dashed grey lines in Fig. 2). As a result, we noted how the Hercules and Hyades lines follow this trend quite closely, whereas Sirius does not. By taking the mean L_z of lines L5 and L9, we estimated the pattern speed of the bar using the Eq. 6 from [15], which yields $\Omega_b \sim 54$ $\mathrm{km\,s^{-1}kpc^{-1}}$. This estimate is consistent with previous values [3, 15] and would correspond to a fast bar.

We also observe some lines that do not cross the SN, meaning that extra-solar MGs exist in other Galactic neighbourhoods. It is not the case of L14 to L17, which are the continuation of L2 and are related to the aforementioned arch 1 (A1, see Fig. 1).

5 Discussion and conclusions

With the study of the 6D *Gaia* DR2 data using the WT we have clearly seen that the classic MGs are part of elongated features, or arches, and have a continuity outside the SN. Some of the structures present a roughly constant energy at a given volume and are probably related with the phase-mixing mechanism, while others evolve with radius at a nearly constant angular momentum, which is to be expected in resonances. As a result, with this new and unprecedentedly accurate data we can now classify each structure and study their dynamical origin in detail. In particular, the characteristics and evolution of the Hercules MG is consistent with the outer Lindblad resonance (OLR) 2:1 models, in which case its pattern speed is ~ 54 $\mathrm{km\,s^{-1}kpc^{-1}}$. Nonetheless, some of the arches observed in the SN above Sirius MG could be caused by the 4:1 OLR of a slow bar [10].

Future data releases will improve the quality and spatial extension of the data, allowing to further explore the kinematic substructure of our Galactic disk. Nonetheless, with this work we have shown that it is already possible to explore as never before both numerical and theoretical models and, thus, gain new insights into the dynamics of the MW.

Acknowledgments

This work has made use of data from the European Space Agency (ESA) mission Gaia, processed by the Gaia Data Processing and Analysis Consortium (DPAC). Funding for the DPAC has been provided by national institutions, in particular the institutions participating in the Gaia Multilateral Agreement. This project has received funding from the University of Barcelona's official doctoral program for the development of a R+D+i project under the APIF grant and from the European Union's Horizon 2020

research and innovation programme under the Marie Skłodowska-Curie grant agreement No. 745617. This work was supported by the MINECO (Spanish Ministry of Economy) through grants ESP2016-80079-C2-1-R (MINECO/FEDER, UE) and ESP2014-55996- C2-1-R (MINECO/FEDER, UE) and MDM-2014-0369 of ICCUB (Unidad de Excelencia 'María de Maeztu').

References

[1] Antoja, T., Figueras, F., Fernández, D., & Torra, J. 2008, A&A, 490, 135

[2] Antoja, T., Helmi, A., Bienayme, O., et al. 2012, MNRAS, 426, L1

[3] Antoja, T., Helmi, A., Dehnen, W., et al. 2014, A&A, 563, A60

[4] Antoja, T., Valenzuela, O., Pichardo, B., et al. 2009, ApJ, 700, L78

[5] Bailer-Jones, C. A. L. 2015, PASP, 127, 994

[6] Binney, J., Gerhard, O., & Spergel, D. 1997, MNRAS, 288, 365

[7] Dehnen, W. 1999, AJ, 118, 1190

[8] Gaia Collaboration, Brown, A. G. A., Vallenari, A., et al. 2018a, A&A, 616, A1

[9] Gaia Collaboration, Prusti, T., de Bruijne, J. H. J., et al. 2016b, A&A, 595, A1

[10] Hunt, J. A. S. & Bovy, J. 2018, MNRAS477, 3945

[11] Katz, D., Sartoretti, P., Cropper, M., et al. 2018, ArXiv e-prints, arXiv:1804.09372

[12] Gómez, F. A., Minchev, I., Villalobos, Á., O'Shea, B. W., & Williams, M. E. K. 2012, MNRAS, 419, 2163

[13] Kushniruk, I., Schirmer, T., & Bensby, T. 2017, A&A, 608, A73

[14] Minchev, I., Quillen, A. C., Williams, M., et al. 2009, MNRAS, 396, L56

[15] Quillen, A. C., De Silva, G., Sharma, S., et al. 2018, MNRAS

[16] Ramos, P., Antoja, T., Figueras, F., 2018, ArXiv e-prints, arXiv:1805.09790

[17] Reid, M. J., Menten, K. M., Brunthaler, A., et al. 2014, ApJ, 783, 130

[18] Schönrich, R., Binney, J., & Dehnen, W. 2010, MNRAS, 403, 1829

[19] Starck, J.-L. & Murtagh, F. 2002, Astronomical image and data analysis, ed. Starck, J.-L. and Murtagh, F. (Springer)

[20] Xia, Q., Liu, C., Xu, Y., et al. 2015, MNRAS, 447, 2367